Ayman Mohammed Ibrahim, Imran Mohd Ibrahim, Noor Azwan Shairi

Centre for Telecommunication Research and Innovation (CeTRI), Fakulti Kejuruteraan Elektronik dan Kejuruteraan Komputer (FKEKK), Universiti Teknikal Malaysia Melaka (UTeM), Melaka, Malaysia

doi:10.15199/48.2020.12.03

Compact Crescent Slot MIMO Antenna with Quad Bands and High Isolation for LTE and 5G communications

Abstract. *A new small crescent MIMO antenna with dimensions of the antenna 31 × 31 × 0.8 mm within the bands of (2.5-2.7, 3.6-4.2, 4.4-4.5, and 5.15-5.6) GHz was designed, and the fabrication and measurement outcomes derived from the use of the MIMO prototype revealed that the crescent MIMO antenna. The small and simple crescent antenna demonstrated high isolation of less than -13.5, -10.5, -15.5 and -29.5dB and envelope correlation coefficient less than 0.01, 0.0024, 0.0008 and 0.0011 respectively. These attributes are suitable for LTE and 5G communications, which is being introduced into China and Japanese markets.*

Streszczenie. Przedstawiono nowy typ małej anteny MIMO o wymiarach *31 × 31 × 0.8 mm i paśmie (2.5-2.7, 3.6-4.2, 4.4-4.5, and 5.15-5.6) GHz. Antena została zaprojektowana, wykonana I zbadana. Antena może być stosowana w aplikacja LTE 5G (**Kompaktowa półksiężycowa antena MIMO do zastosowań LTE 5G**).*

Keywords: 5G band, Envelope correlation coefficient (ECC), isolation, MIMO antenna, mutual coupling.
Słowa kluczowe: antena MIMO, pasmo 5G, LTE

Introduction

With the development of fifth-generation mobile communication, the requirements for a high-quality and high data rate increase. Multi-input multi-output mobile communication has many applications including 5G. Later work is concentrating on even more antennas to improve the small size and high isolation further in the fifth generation. To obtain reliable performance in a Multi-input multi-output communications system, one demand is that the correlation coefficients between the signals received by the MIMO antenna ports are adequately low[1]–[5]. The signal correlation between the antenna ports is divided into two separate effects, the first because of the mutual coupling between antennas and the second being that due to channel correlation. Also, the impact of mutual coupling will change the antenna patterns and hence the channel correlation[6]–[10].

Thus, one of the challenges of designing MIMO communication antennas is to provide sufficiently high antenna isolation. It is difficult to achieve the design of small MIMO antennas with high isolation and there are known basic limits for the design numbers of antennas in a specific area or size. Therefore, designs that could approach these limits are of interest, and in the previous works on the design of the MIMO antenna, there was a large variety of methods. The focus on smart device miniaturization would require less space for antenna design, and consequently, this will affect the close association between isolation and bandwidth in the MIMO antenna system. As such, this paper attempted to solve the above-mentioned issues with high isolation printed on two-element arrays operating bands of (2.5-2.7, 3.6-4.2, 4.4-4.5, and 5.15-5.6) GHz.

Antenna Design

The cell of the proposed antenna is a rectangular antenna with the design process undertaken in five stages. In the first stage (see fig.1-a), the process begins with designing a rectangular shape antenna (antenna1) with dimensions 13 × 18 mm2. The opriting frequency of the rectangular antenna is calculated by[10], [11]:

$$f_r = \frac{c}{2L\sqrt{\epsilon_r}} \quad (1)$$

In the second stage, it designed a slot circle-shaped with a radius of C1 = 5.5 mm. In Fig.1-b, it created the antenna2 from combine antenna1 and slot designed. In the third stage, the circular C3 can be designed via cutting a circular slot that a radius of 3.5 mm in the patch plane (antenna3) and combine with circle C2 that a radius of 4.5 to create antenna4. In the last stage, the rectangular antenna (antenna5) is designed to combine the characteristics of a circular antenna 3 and a rectangular antenna by creating an antenna 4, as shown in Fig.1-c.

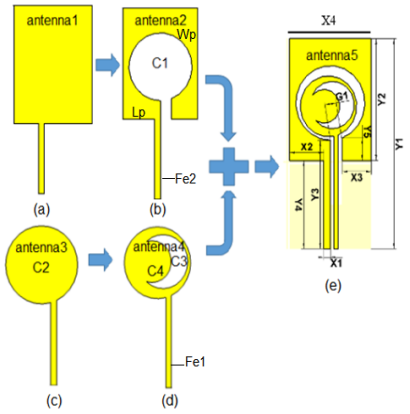

Fig. 1: The crescent slot MIMO antenna configuration process

In Fig.1-e, The total length of all arms of the modified patch can be calculated, as follows:
The upper arm of length of X4 = 13 mm.
The right arm of length Y2 = 13.5 mm.
The left-arm of length is Y2=13.5 mm.
The lower arm length is: X3+ Y5+ (2 × π × r – G1) +Y3-Y4+ X2 = 4.615 + 3.3 + 2 × π × 5.5 - 1.817 + 16 – 13 + 5.415 = 49.053.
Each arms in modified the perimeter patch is:
=13 + 13.5 + 13.5 + 49.053 = 89.053mm.

The term (2L=k) in equation (1) represents half perimeter of the rectangular patch, So equation (1) can be rewrites as[6], [9]:

$$f_r = \frac{c}{K\sqrt{\epsilon_{eff}}} \quad (2)$$

however

$$\frac{the\ perimeter\ of\ modified\ patch}{the\ perimeter\ of\ rectangular\ patch} = \frac{89.053}{53} = 1.68\ \text{mm}$$

thus, (2) can be modified to the following form :

$$f_r \approx \frac{c}{1.68\,K\sqrt{\epsilon_{eff}}} \quad (3)$$

The cell geometry of the suggested MIMO antenna is shown in Fig.1. The movement of current in the patch plane was accomplished by a method of two lines, formed by antenna 1 (Fe1–C3–C4) and antenna 2 (Fe2–Lp–Wp), printed on the patch plane, and formed by length of slot L16, printed on the ground plane. The required resonant frequency, suggested for MIMO antenna, was adjustable by altering the length of slot L16. These dimensions were optimized through the CST simulation program as Fe1 = 16.78 mm and L11 = 2mm. While C3 and C4 were circles with radius of 4.5mm and 2.5mm respectively.

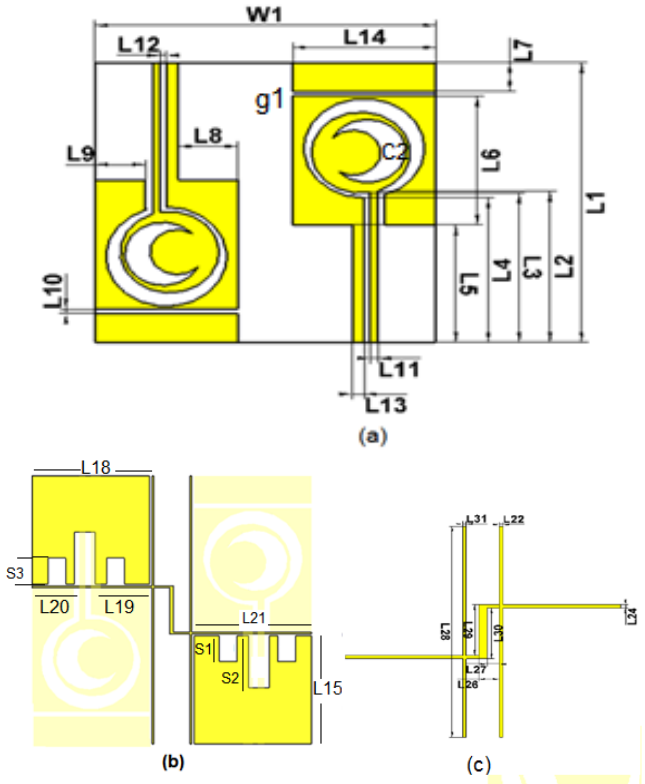

Fig. 2: The proposed design geometry of the crescent slot MIMO antenna, (a) Front view, (b) back View and (c) naturalization technique.

The dimensions of the second line were to be Fe2 = 10, L13 = 6, Lp = 40 and Wp = 40 mm. The circle C1 was designed by cutting a circular slot having radius of 5.5 mm in the patch plane Wp − Lp, while the crescent shaped circular slot C2 was designed by cutting a slot with radius of 3.5 mm in circle C4. The suggested antenna was configured by combining antenna4 and antenna2. The configuration process for two antennas is shown in Fig. 1. The size of the ground plane is given by, L15 = 12.6 mm × L16 = 13mm, which lies at the bottom end of the suggested MIMO antenna, where the rectangular slot for control of resonant bands is located , in as shown Fig.2. The dimensions of the proposed MIMO antenna are mentioned in Table 1. Radiating elements of the two-element MIMO antenna design have a symmetric monopole antenna, fed by a 50 Ω microstrip line. This proposed MIMO antenna includes two separate ports with a distance of 5 mm, monopoles printed on a 31 × 31 mm (FR-4) substrate with a copper thickness of 0.035 mm, a dielectric constant of 4.3 and a FR4 substrate with thickness of 0.8 mm, as exhibited in Fig. 2. In order to obtain high isolation, neutralization lines were inserted between the two separate antennas, on the ground plane using defected ground structure on the inserted slot in the ground plane. This complements the two vertical lines of width, L22= 0.55 and length, L31=0.2 and the two horizontal lines of width, L24 = 0.2 and length L = L18+ L22 + L26 - L27= 13.6, which intersect with another vertical line of width, L27 - L26 = 0.4 and length, L30 + L24 = 5.6, and a slot of length, (L16 +L17+ L16) = 14.3mm, as shown in Fig. 2(c).

Table 1: Parameters and dimensions of the crescent slot MIMO antenna (mm)

parameter	value	parameter	value	parameter	value
L1	31	L13	1.09	L25	0.2
L2	12.78	L14	13	L26	2.2
L3	16.58	L15	12.5	L27	1.8
L4	16	S2	6	L28	31
L5	13	L17	2.3	L29	5.4
L6	14.3	L18	13	L30	5.4
L7	8.2	L19	6	L31	0.2
L8	5.42	L20	4.7	C1	5.5
L9	4.61	L21	13	C2	3.5
L10	0.5	L22	0.2	C3	2.5
L11	0.7	L23	0.3	W1	31
L12	0.55	L24	0.2	-	-

Antenna Parametric analysis

The computer simulation reflection coefficient was used to study the effect of variation in the dimensions of the radiating element slots s1, s2, s3, circle c2 and the gap g1.

1. Effect length of the slot S1

In order to illustrate the effect of variation in the structure technique on the production of operating bands, the proposed antenna was simulated with various S1 values. The simulated S-parameter values are exhibited in Fig. 3. The difference in results of the proposed MIMO antenna used in the LTE and 5G applications, suggests the influence of the varying S1 lengths on the various dual bands of LTE and 5G. By fixing the other radiation elements including the length of Lg= 3.2 mm and Lf = 17.78 mm, and varying the length of the slot S1, the impedance of ground plane of the antenna was changed due to variation in the size of the U-slot S1. In Fig. 3, the solid curve represents the return losses of the antenna when the length of slot S1 was 9 mm. As shown in Fig.3 (a), when the S1 length is 9 mm, operating band ranged 3.2 - 6.3 GHz. By changing the length of slot S1 to 6 mm, the operating band splits into two narrow bands with the frequency ranges of 3.4 - 3.6 GHz and 5.15 - 5.925 GHz. When the length of slot S1 is changed to 0.5 mm the operating bands ranges are 3.15 - 3.55 GHz and 4.4 - 4.99 GHz. For the first operating band, by changing the value of the length of slot S1 from 6 mm to 0.5 mm, the isolation increases from -10 dB to -12 dB, as indicated by the blue and black curves, respectively in Fig. 3 (b). For the second operating band, the isolation value remain unchanged at -19 dB for both lengths of slot S1, as shown in Fig. 3 (b).

For radiation elements with, length of Lf = 8.2 mm and Lg = 12.78 mm, and by varying the length of the slot S1, the diameter of part ground plane of the antenna was changed due to change in the size of the U-slot S1. It can be observed from Fig. 4 that the return loss and isolation curves differ significantly according to various lengths of slot S1. In Fig. 4, the solid curve represents the return losses of the antenna, while the dashed curve represents the isolation values. All other radiation elements were fixed and only U-shaped slot S1 in the ground plane was varied. In Fig. 4 (a), the solid red curve represents the return losses of

the antenna when the length of slot S1 = 5 mm, with three operating bands ranging 2.5 - 2.7 GHz, 3.4 - 4.2 GHz and 4.6 - 5.3 GHz. The third operating band splits into two narrower bands around the frequency ranges of 4.05 - 4.4 GHz and 4.8 - 5.545 GHz. With the length of slot S1 = 3 mm, four operating bands ranging 2.5 - 2.7 GHz, 3.4 - 3.8 GHz, 4.05 - 4.4 GHz and 4.8 - 5.45 were obtained, as indicated by the solid blue curve. In Fig. 4 (a), the black curve shows the four operating bands resulted from the length of the slot S1 = 1 mm, two of which can be used for 5G applications and other two can be used for LTE applications. Fig. 4 (b) indicates the influence of the varying lengths of S1 on the various isolation. This influence led to a high isolation level of about -13.5 dB, -10.5 dB, - 15.5 dB and -29 dB in the bands ranging 2.5 - 2.7 GHz, 3.6 - 4.2 GHz, 4.4 - 4.5 GHz and 5.15 - 5.6 GHz respectively.

Two observations are obtained from above discussion. Firstly, the change in length of slot S1 leads to change in the path length of the surface current and thus the resonant frequencies vary in a dramatic way while the length of slot S1 exclusively effects the frequency bands ranging 3.4 - 5.6 GHz. Secondly, the variation in the length of slot S1 effects the isolation of the proposed MIMO antenna on all bands.

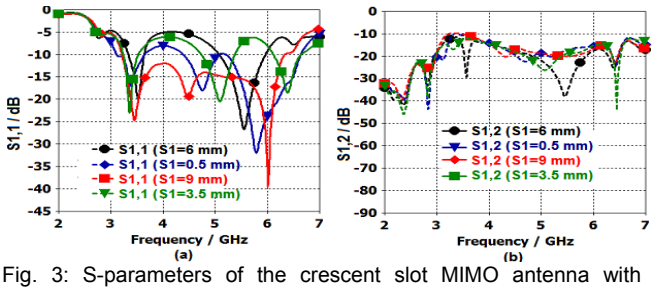

Fig. 3: S-parameters of the crescent slot MIMO antenna with changing values of S1 while fixing Lg= 3.2 mm and Lf = 17.78 mm. (a) Simulated return loss (b) Simulated isolation

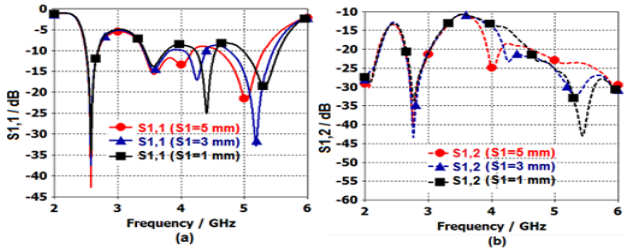

Fig. 4: S-parameters of the crescent slot MIMO antenna with changing values of S1 while fixing Lg= 8.2 mm and Lf= 12.78 mm. (a) Simulated return loss (b) Simulated isolation

2. Effect of the slots S2

By fixing the other radiation elements except lengths Lg = 8.2 mm, Lf = 12.78 mm and changing the length of slot S2, the diameter of part ground plane of antenna is changed due to change in the size of the slot S2. It can be observed in Fig. 5 that the return loss and isolation curves differ significantly at various lengths of slot S2. The solid black curve represents the return losses of the antenna when the length of slot S2 = 1 mm, with two operating bands (3.15 - 3. 55 GHz and 4.45 - 6.65 GHz). When the length of slot S2 is changed to 3.5 mm, second operating band splits into two narrow bands with frequency ranges of 4.4 - 4.99 GHz and 5.2 - 6.65 GHz, to become three operating bands 3.15 - 3.55 GHz, 4.4 - 4.99 GHz and 5.2 - 6.65 GHz, as indicated by the solid red curve. In Fig. 5 (a), the blue curve observed two operating bands resulting from the length of the slot S2 = 4 mm. Fig. 5 (b) indicates the influence of the varying S2 lengths on the various isolation values for different operating bands. This influence led to a high isolation level of about -10.5 dB, -20 dB and -15 dB in the three bands.

By fixing the radiation elements, lengths of Lg = 3.2 mm and Lf = 17.78 mm and changing the length of the slot S2, the diameter of part ground plane of antenna changes due to change in the size of the rectangular slot S2. As shown in Fig. 6, the return loss and isolation curves vary significantly according to the different locations of slot S2. In Fig. 6 (a), two operating bands ranging 3.3 – 3.7 GHz and 5.1 – 5.9 GHz are shown with length of slot S2 as 2.5 mm. By changing the length of slot to S2 = 6 mm, the second operating band disappears, while the first operating band splits into two narrow bands with frequency ranges of 3.3 - 3.7 GHz and 5 - 5.85 GHz. With the length of slot S2 = 1.5 mm, the return losses are decreased from -30 dB to -58.5 dB for the resonant frequency, as indicated by the red curve. As shown in Fig. 6 (b), the change in length of slot S2 to 1 mm, the isolation of the crescent slot MIMO antenna in 1st band and 2nd bands is unchanged (-12.5 dB and -20 dB).

These observations lead to following two conclusions. Firstly, changing the slot S2 length leads to a change in the path length of the surface current, and thus the resonant frequencies, that allow it to function in two operating bands for 5G applications. The length of slot S2 exclusively affects 3.1 - 3.55 GHz and 4.4 -4.99 GHz frequency bands. Secondly, isolation of crescent slot MIMO antenna is greatly not affected by change in the length of slot S2.

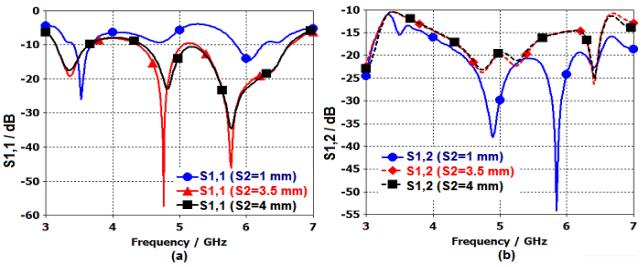

Fig. 5: S-parameters of the crescent slot MIMO antenna with changing values of S2 while fixing Lg = 8.2 mm, Lf = 12.78 mm. (a) Simulated return loss (b) Simulated isolation

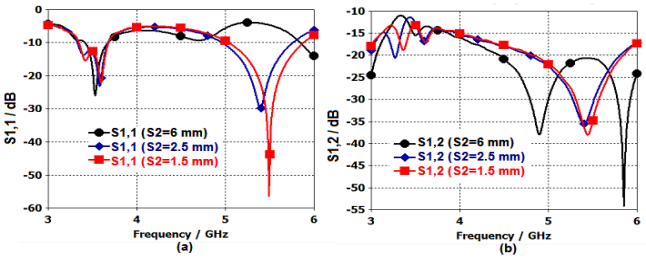

Fig. 6: S-parameters of the crescent slot MIMO antenna with changing values of S2 and fixing S1= 6 mm, Lg = 3.2 mm and Lf = 17.78 mm. (a) Simulated return loss (b) Simulated isolation

3. Effect of the slot S3

By fixing all the radiation elements, length of Lf = 8.2 mm, Lg = 12.78 mm, S1= 0.5 mm and changing the length of the slot S3 to the down side in the ground plane, the diameter of part ground plane of antenna changes due to change in the size of the slot S3. Additionally, the return loss and isolation curves also varies as the length of slot S3 is changed. In Fig. 7 (a), the red curve represents the return losses of the antenna when the length of the slot S3 = 1 mm. At this length, two operating bands, 3.27 - 3.44 GHz and 4.44 - 4.88 GHz, are observed. When the slot length is changed to 6 mm, a third operating band appears, and the operating ranges 3.15 - 3.55 GHz, 4.4 - 4.99GHz and 5.21 -

6.62 GHz, as indicated by the black curve. In Fig. 7 (a), the blue curve observed three operating bands, when the length of the slot S3 is changed to 0.5 mm. Fig. 7 (b) indicates the influence of the change in S3 lengths on the various isolation values for first and second operating bands. The variations lead to high isolation levels of about -10.5 dB and -20 dB, in the two 5G bands mentioned above.

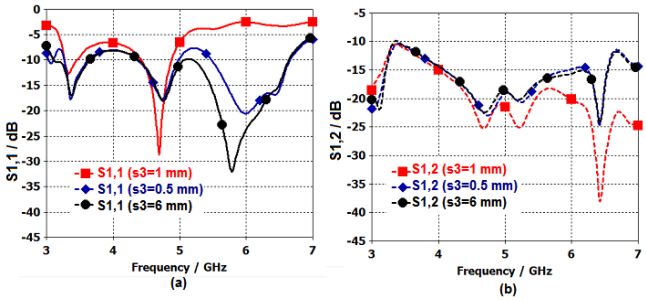

Fig. 7: S-parameters of the crescent slot MIMO antenna with changing values of S3 and fixing S1= 0.5 mm, Lg = 8.2 mm and Lf = 12.78 mm. (a) Simulated return loss (b) Simulated isolation

By fixing all the radiation elements, length of Lf = 3.2 mm, Lg = 17.78 mm and changing the length of the slot S3 to the down side in the ground plane, the diameter of part ground plane of antenna changes due to change in the size of the slot S3. As shown in Fig. 8, the return loss and isolation curves vary significantly according to the different locations of slot S3. As shown in Fig. 8 (a), there are two operating bands (3.1 - 3.42 and 5.08 - 5.91 GHz) when the length of slot S3 is 1.5 mm. As the length of slot S3 is changed to 5 mm, the first operating band disappears, while the second operating band splits into two narrow bands around the frequencies range of 3.15 - 3.55 GHz and 5.15-5.925 GHz. At length S3 = 0.5 mm, with a decrease in value of return loss for a second band. For 0.5 mm and 1.5 mm slot lengths, the value of return losses for the resonant frequency ranges from -25 dB to -33.5 dB, as indicated by the blue and red curves. In Fig. 8 (b), by changing the length of slot S3 to 0.5 mm, the isolation of the crescent slot MIMO antenna in first and second band is changed to -13 dB and -18 dB respectively.

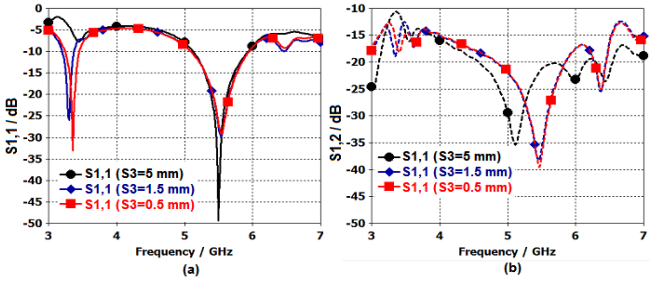

Fig. 8: S-parameters of the crescent slot MIMO antenna with changing values of S3 and fixing S1= 6 mm, Lg = 3.2 mm and Lf = 17.78 mm.(a) Simulated return loss (b) Simulated isolation.

The above observations lead to following two conclusions. Firstly, changing the slot S3 length leads to a change in the path length of the surface current, and thus the resonant frequencies, that allow it to function in two operating bands for both LTE and 5G applications. The length of slot S3 exclusively affects 3.1 - 3.55 GHz and 4.4 - 4.99 GHz and 5.15 - 5.925 GHz frequency bands. Secondly, isolation of crescent slot MIMO antenna is greatly affected by change in the length of slot S3.

4. Effect of the slot C2

By fixing the other radiation elements and shifting the center of the circle C2 to the left or upper, the patch plane changes due to change in the position of the crescent slot C2. As shown in Fig. 9, the return loss curve significantly varies for different locations of circle C2. The solid curve represents the return losses of the antenna when the center of circle C2 is at point (0.4, 11.5) in the (x-y) plane. In Fig. 9 (a), three operating bands dual (3.2 - 3.6 GHz and 5.1 - 5.95 GHz; 3.4 - 3.65 GHz and 5.15 - 5.925 GHz; 3.34 - 3.64 GHz and 5.1 - 5.99 GHz) are achieved when the circle C2 is moved to the left and up side. While, when the center of the circle C2 is at point (0.4,11.5), it generates two operating bands dual (3.34 - 3.64 GHz and 5.1 - 5.99 GHz) and a single operating band (2.7 - 3.3 GHz) when the circle C2 is moved to point (0.4,12) (see Fig. 9 (a)). In Fig. 9 (a), by shifting the center of circle C2 to point (0.4,12), the second operating band disappears,, while the first operating band shifted to the right, as indicated by the black curve. When point C2 is shifted (0.4,12) to (0.6,11.5) (see Fig. 9 (b)), the isolation of the proposed MIMO antenna is changed from -32 dB to -25 dB in both operating bands. In Fig. 9 (a), by shifting the center of the circle C2 from C2 (0.6,12) to point (0.4,11.5), the second operating band is unchanged, while the return losses for the resonant frequency are changed from -20.5 dB to -25 dB. By shifting the center of circle C2 to point (0.6,11.5) to (04, 11.5), the first operating band range shifts from 3.2 - 3.6 GHz to 3.4 - 3.6 GHz. When center of point C2 is shifted from (0.4,11.5) to (0.6,11.5), the isolation of the proposed MIMO antenna changes from (-11.5, -19) dB to (-12, -20.5) dB in both operating bands.

The above paragraph demonstrates that a change in circle C2 location leads to change the size of the Crescent slot C3 which leads to change the path length of the surface current and thus, the resonant frequencies in both first and second operating bands. The location of circle C2 is exclusively affected the frequency bands 3.4 - 3.65 GHz and 5.15 - 5.925 GHz.

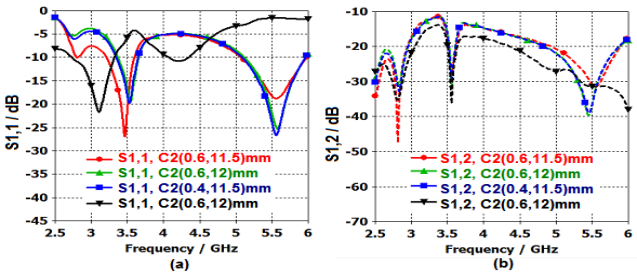

Fig. 9: S-parameters of the crescent slot MIMO antenna with changing values of C2 while fixing S1= 0.5 mm, Lg= 3.2 mm and Lf= 17.78 mm. (a) Simulated return loss (b) Simulated isolation.

5. Effect of the gap g1:

By fixing the other radiation elements and changing the length of slot g, the impedance of an antenna changes due to change in the size of the rectangular slot g1. As shown in Fig. 10, the return loss and isolation curves significantly varies for the different sizes of the slot g1.

In Fig. 10 (a), there are two operating bands (3.34 - 3.64 GHz and 5.15 - 6.17 GHz) when the length of slot g1 is 2.5 mm. By removing the slot g1 all together (g1 = 0 mm), disappears of the first operating band, when slot g1 changed 0 to 1mm, the second operating band splits into two narrow bands with the frequency ranges of 3.34 - 3.64 GHz and 5.15 - 5.925 GHz. At length g1 = 2.5 mm, return losses for the resonant frequency decreases from -30 dB to -48 dB, as indicated by the black and red curves. In Fig. 10 (b), by changed the length of slot g1 from 2.5 to 1 mm, the isolation of the proposed MIMO antenna in the first and second band is unchanged (-11.5 dB and -18 dB respectively).

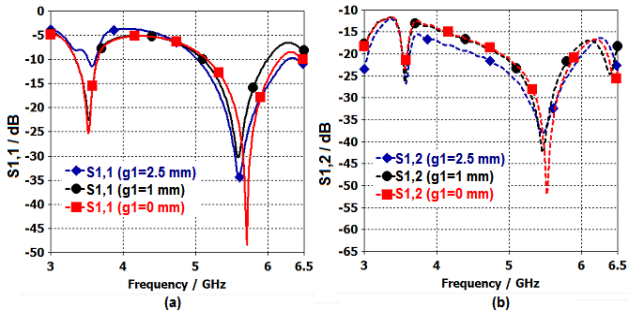

Fig. 10: S-parameters of the crescent slot MIMO antenna with changing values of the gap g1 while fixing S1= 0.5 mm, Lg = 3.2 mm and Lf = 17.78 mm. (a) Simulated return loss (b) Simulated isolation

By fixing the other radiation elements and changing the two parameters, U-shaped slot S1 in ground plane and slot g1 in the patch plane, the impedance of the antenna is affected. As shown in Fig. 11, the return loss and isolation curves significantly varies for different length of slots g1and S1. In Fig. 11 (a), the solid red curve represents the return losses of the antenna when the lengths of slots g1 and S1 are 0.2 mm and 1.7 mm, respectively, two operating bands 2.6 - 2.7 and 3.5 - 5.4 GHz are observed. The second operating band splits into two narrow bands around the frequency ranges of 3.4 - 4.2 GHz and 4.6 - 5.3 GHz when the length of slot S1 is changed to 5 mm, to get three operating bands, as indicated by the blue curve. In Fig. 11 (a) the third operating band splits further to two narrow bands around the frequency ranges of 4.3 - 4.6 GHz and 5.1 - 5.6 GHz when the length of S1 is reduced to 0 mm, to get four operating bands 2.5 - 2.7 GHz, 3.4 - 3.8 GHz, 4.3 - 4.6 GHz and 5.12-5.6 GHz, as indicated by the black curve. Fig. 11 (b) indicates the influence of the varying the length of g1 on various bands of LTE and 5G. This influence lead to high isolation levels of about -13.5 dB, -10.5 dB, -15 dB and -28 dB, in the four bands mentioned above.

The above observations leads to following two conclusions. Firstly, changing the slot g1 length leads to change the path length of the surface currents and thus the resonant frequencies, for all the four operating bands. The length of slot g1 is exclusively affected in the frequency bands 2.5 - 2.7 GHz, 3.4 - 3.8 GHz, 4.4 - 4.7 GHz and 5.15 - 5.65 GHz. Secondly, change in the length of slot g1 does not effect the isolation of the proposed MIMO antenna.

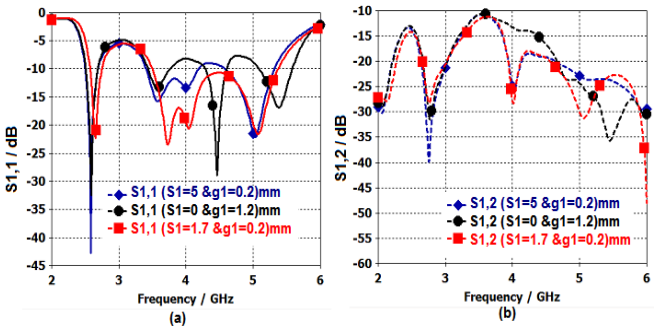

Figure 11: S-parameters of the crescent slot MIMO antenna with changing values of the gap g1 and S1, while fixing Lg = 8.2 mm and Lf = 12.78 mm (a) Simulated return loss (b) Simulated isolation.

Performances MIMO antenna

1. Isolation technique

In order to obtain high isolation, using defected ground structure to the inserted slot on the ground plane and neutralization lines were inserted between the two separated antenna on the patch plane. Firstly, the defected ground structure used three U-shaped of slots (S1, S2 and S3). The effects of the S1, S2 and S3 slots lengths, on the frequency response and bandwidth, were explained through a parametric study. This study revealed that an increase, or decrease, in the S1, S2 and S3 ground plane slots width values, induced a change in the centre resonant frequency of the design bandwidth. This indicates that the width of the slots is highly sensitive towards the MIMO antenna design. Secondly, the neutralization lines used two vertical lines of width L12= 0.55 and length L=31, and the two horizontal lines of width L24 = 0.2 and length L16 = 13, which intersect with another vertical line of width L32=L27 - L26 = 0.4. The neutralization lines reduce the coupling and the defected ground structure in the ground plane further reduce the coupling and thereby increases the isolation between the antenna elements. The antenna elements are placed symmetrically between them distance 5 mm and this enhances the isolation between the MIMO antenna elements. In Fig.12 shown, the current in the input element is taken at a specific location where the impedance is at the minimum and the current at the maximum, and then its phase is reversed by hybrid isolation technical. This reverse current is fed to the nearby antenna to reduce the amount of coupled current. The neutralization line is Four intersecting lines with three slots in the ground plane, which improves isolation between the antenna elements and solves the problem of mutual coupling.

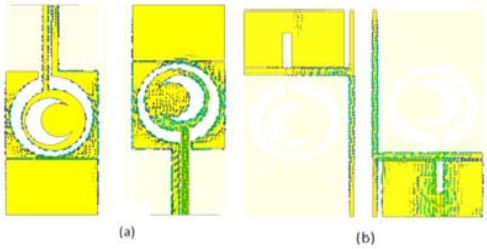

Fig.12: Simulated current densities at 5.5375 GHz central frequency of the (5.15-5.925) band of (a)Front view (b) Back view

2. ECC and Efficiency

In Fig.13 shown, the envelope correlation coefficient of the MIMO antenna with port-1. The maximum ECC obtained (0.01, 0.0024, 0.0008 and 0.001) of the quad bands (2.5-2.7, 3.4-4.2, 4.4-4.5 and 5.15-5.6) GHz when S1=1 mm. while, when S1=6 mm, the maximum ECC obtained (0.012 and 0.0056) of the dual bands (3.15-3.55 and 4.4-4.99) GHz.

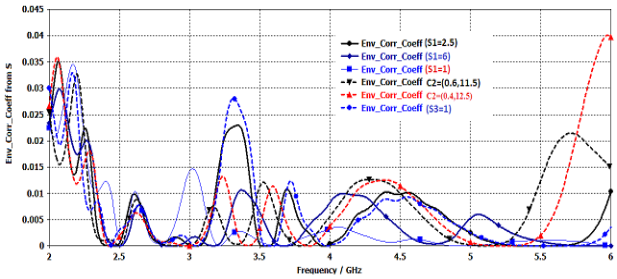

Fig. 13: Envelope correlation coefficient of the crescent MIMO antenna

When changing the value of S1=2.5 mm, the ECC is decreased from 0.024 to 0.02 at the 1st band (3.4-3.6) GHz. When S3 = 2 mm, lead to the envelope correlation coefficient values are decreased at 1st band (3.15-3.52) GHz and increased at 2nd band (5.15-5.925) GHz. In Fig.14 shown, for the antenna efficiency, it is above 55% in

the operation bands (3.4 - 3.6) GHz, (3.15 - 3.50) GHz, (4.4-4.49) GHz and (3.4 - 4.2) GHz. where other bands too achieved the requirement antenna efficiencies. A summary of the operating frequencies, envelope correlation frequency and the efficiency values arising from changes in the parameters (S1, S3 and C2) of the above of the results, is portrayed in Table 2.

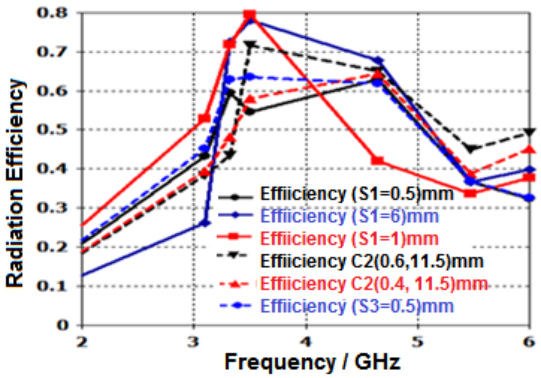

Fig. 14: Efficiency of the crescent MIMO antenna

Table 2: A summary of the efficiency, ECC and isolation of the crescent MIMO antenna

BW (GHz)	fr.	Efficiency %	ECC	Isolation
2.5-2.7	2.6	39-44	< 0.01	-13.5
3.6-4.2	3.8	58-80	< 0.0024	-10.5
4.4-4.5	4.4	45-50	< 0.0008	-15.5
5.15-5.6	5.2	37-40	< 0.0011	-29.8

Prototype and Measurement result

A MIMO antenna three prototypes were fabricated for the quad bands (2.5-2.7 - 3.4-4.2 - 4.4-4.5 and 5.15-5.6) GHz. In Fig.15 shown, the fabrication of these antenna prototypes involved the use of an inexpensive FR4 dielectric, with an overall dimension of 31 × 31 × 0.8 mm. As illustrated in Fig.15, the simulated and measured reflection and transmission coefficients demonstrated by the two representatives of the MIMO antenna indicate that their performance levels are identical. The results of the proposed antenna are shown from Fig.16 (a), which A panoramic network analyzer (PNA-5227A) was used to measure the S-parameters of the proposed antenna. Substantial agreement in bandwidth and isolation was observed between simulated data (the black colour) and measured data (the red colour). The disparity between simulated data and measured data can be put down to the impurity of materials utilized in the prototype, the solder between an FR4 material and connector SMA, as well as the disregard for the impedance of the connectors and cables during the simulation.

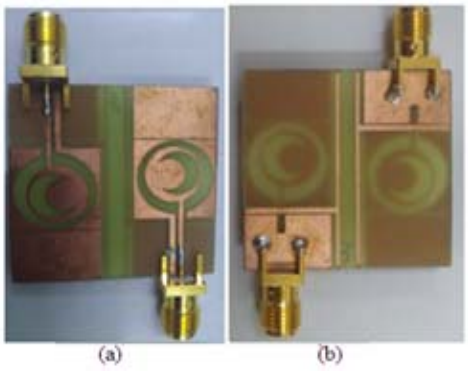

Fig. 15: A photograph of the three fabricated antennas (a) Front of the MIMO antennas (f) Back of the MIMO antenna

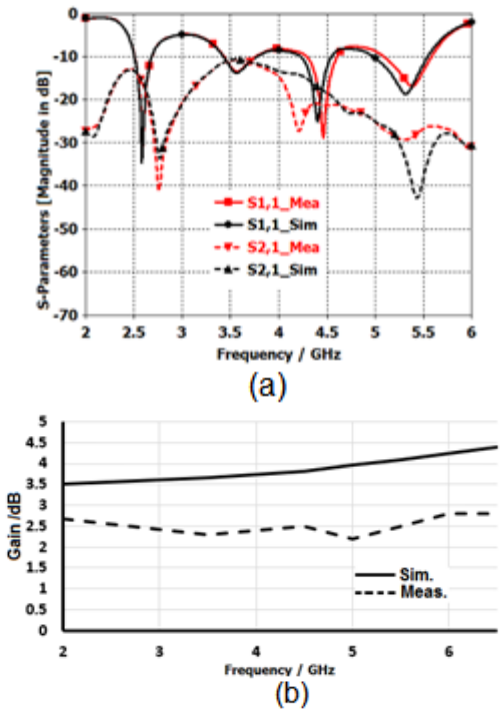

Fig. 16: The simulated and measured S-parameters of port 1 (a) S-parammeter of antenna (b) Gain of antenna

Further, A panoramic network analyzer (PNA-N9020A), vector signal generator (E8267D) and horn antenna were used to measure the gain of the fabricated antenna. In Fig.16(b), suitable agreement in gain was observed between simulated data (the solid) and the measured data (the dashed).

Validation of the Proposed Antenna

Table 3 shows, the comparison of findings between this research work with other research work. The proposed antenna is compared with several selected types of research. The comparison was based on important characteristics, such as a number of ports, isolation, efficiency, envelope correlation coefficient, material, bandwidth and size. This MIMO antenna is the best for LTE and 5G communications propose for several reasons.

The first reason is the fact that MIMO Antenna has quad operating bands that cover all required frequencies for LTE and 5G communications 2.5-2.7, 3.6-4.2, 4.4-4.5, and 5.15-5.6) GHz. The second reason is high isolation and very small size. The Third reason is envelope correlation coefficient properties at some operating bands for MIMO Antenna that has is less than 0.01, 0.0024, 0.0008 and equal 0.0011 of the four bands respectively. The fourth reason is a small size, which provided the possibility of using the proposed MIMO antenna for mobile LTE and 5G communications devices. The Fifth reason is that fact that side from being low cost, ease of fabrications and use of commercial FR-4 substrate, the antennas examined in this study can be adopted for the purpose for which that has designed.

The selection criteria for other research work are Isolation, size, efficiency, Envelope correlation efficient and material used. It is found that the proposed antenna has high isolation, small size efficiency and ECC meet the requirement for using 5G applications.

Table 3: Comparisons between the proposed of MIMO antennas and previous related antennas

Ref.	BW (GHz),	Size (mm^2)	Iso.	ECC	Effi. (%)
[12]	(2.4-2.5) (5.15- 5.35)	110 × 55	-15	< 0.02	> 70
[13]	(2.4–2.48) (3.4–3.8) (4.7–5.83)	60 × 25	-15	< 0.16	52-88
[14]	(2.4-2.5) (5.15-5.35)	55 × 65	-15	< 0.15	60-65
[15]	(2.1-2.6) (3.2-3.7) (4.8-5.4) (6.6-7.4)	60 × 40	-23	< 0.002	82-89
[16]	(3.6-3.8) (3.9-4.2) (5.1-5.85)	40.5×40.5	-17	< 0.035	40-80
[17]	(2.24-2.5) (3.6-3.99) (4.4-4.6) (5.71-5.9)	37 × 56	-15	< 0.08	49-83
This work	(2.5-2.7) (3.6-4.2) (4.4-4.5) (5.15-5.6)	31 × 31	-13.5 -10.5 -15.5 -29.5	< 0.01 < 0.0024 < 0.0008 < 0.0011	39-44 58-80 45-50 37-40

Conclusion

A mobile phone with a MIMO antenna design was proposed for the use of LTE and 5G MIMO communications. This job involved the simulation and fabrication of a novel MIMO antenna for the band's ranges of (2.5-2.7, 3.6-4.2, 4.4-4.5, and 5.15-5.6) GHz. The different bands were controlled by way of the application of decoupling hybrid technique (neutralization lines and defected ground structure). Besides enhancing the isolation between the antenna ports, the envelope correlation coefficients between the signals received by the MIMO antenna elements was enough reduced to meet the specifications for LTE and 5G applications.

Acknowledgment

The authors would like to thank Centre for Telecommunication Research and Innovation (CeTRI), Research and Innovation Management (CRIM) and Universiti Teknikal Malaysia Melaka (UTeM) for their encouragement and help for supporting financially to complete this research work.

***Authors**: A. M. Ibrahim, Email: ayman971972@gmail.com; I. M. Ibrahim, Email: imranibrahim@utem.edu.my; N. A. Shairi, Email: noorazwan@utem.edu.my. The address for all authors Faculty of Electronics and Computer Engineering, Universiti Teknikal Malaysia Melaka (UTeM), 76100 Durian Tunggal, Melaka, Malaysia.*

REFERENCES

[1] Y. L. Ban, C. Li, C. Y. D. Sim, G. Wu, and K. L. Wong, "4G/5G Multiple Antennas for Future Multi-Mode Smartphone Applications," *IEEE Access*, 2016, 4, (c), pp. 2981–2988.

[2] A. M. Ibrahim, I. M. Ibrahim, and N. A. Shair, "Compact MIMO Antenna for LTE and 5G Applications," *Int. J. Microw. Opt. Technol.,* 2020, 15, (4), pp. 360-368.

[3] A. M. Ibrahim, I. M. Ibrahim, and N. A. Shairi, "A Compact Quad Bands-Notched Monopole Antenna for Ultra-Wideband Wireless Communication," *Religación*, 2019,53,(9), pp. 1689–1699.

[4] A. M. Ibrahim, I. M. Ibrahim, and N. A. Shairi, "A Compact Sextuple Multi-Band Printed Monopole Antenna," *Opción*, 2018, 34, (86), pp. 1448–1467.

[5] L. Sun, H. Feng, Y. Li, and Z. Zhang, "Compact 5G MIMO Mobile Phone Antennas with Tightly Arranged Orthogonal-Mode Pairs," *IEEE Trans. Antennas Propag.*, 2018, 66, (11), pp. 6364–6369.

[6] A. M. Ibrahim, I. M. Ibrahim, and N. A. Shairi, "COMPACT MIMO Slot Antenna oF Dual-Bands for LTE and 5G Applications.," *Int. J. Adv. Sci. Technol.*, 2019,28, (13), pp. 239–246.

[7] H. Alsariera, Z. Zakaria, A. A. M. Isa, O. S. Al-heety, and M. Y. Zeain, "New CPW-fed Broadband Circularly Polarized Planar Monopole Antenna Based on a Couple of Linked Symmetric Square Patches," 2020, 1, (2), pp. 95–103.

[8] H. Alsariera, Z. Zakaria, A. A. M. Isa, S. Alani, M. Y. Zeain, and H. Alsariera, "Simple Broadband Circularly Polarized Monopole Antenna with Two Asymmetrically Connected U-shaped Parasitic Strips and Defective Ground Plane," *Telecommun. Comput. Electron. Control.,* 2020, 18, (3), pp. 1169–1175.

[9] A. M. Ibrahim, I. M. Ibrahim, and N. A. Shairi, "Compact MIMO Slots Antenna Design with Different Bands and High Isolation for 5G Smartphone Applications," *Baghdad Sci. J.*, 2019, 16, (4), pp. 1093–1102.

[10] A. M. Ibrahim, I. M. Ibrahim, and N. A. Shairi, "Compact MIMO Antenna with High Isolation for 5G Smartphone Applications," *J. Eng. Sci. Technol. Rev.*, 2019,12, (6), pp. 121–125.

[11] A. M. Ibrahim, I. M. Ibrahim, and N. A. Shairi, "Design a Compact Wide Bandwidth of a Printed Antenna Using Defected Ground Structure," *J. Adv. Res. Dyn. Control Syst*, 2019,11, (2), pp. 1065–1076.

[12] L. Zhao and K. Wu, "A Dual-Band Coupled Resonator Decoupling Network for Two Coupled Antennas," *EEE Trans. Antennas Propag.*, 2015, 63, (7), pp. 2843–2850.

[13] H. S. Singh, Shalini, and M. K. Meshram, "Printed Monopole Diversity Antenna for USB Dongle Applications," *Wirel. Pers. Commun.*, 2016, 86, (2), pp. 771–787.

[14] N. K. Kiem and D. N. Chien, "A Transmission Line Decoupling Technique for Enhancement of Port Isolation of Dual-Band MIMO Antennas," *J. Electromagn. Waves Appl.*, 2018, 32, (10), pp. 1195–1211.

[15] K. V. Babu and B. Anuradha, "Design of Multi-Band Minkowski MIMO Antenna to Reduce the Mutual Coupling," *J. King Saud Univ. - Eng. Sci.*, 2018,6, (3), pp. 51-57.

[16] I. Suriya and R. Anbazhagan, "Inverted-A based UWB MIMO Antenna with Triple-band Notch and Improved Isolation for WBAN Applications," *Int. J. Electron. Commun. (AEÜ)*, 2019, 99,(5), pp. 25–33.

[17] S. Chouhan, V. S. Kushwah, D. K. Panda, and S. Singhal, "Spider-shaped fractal MIMO antenna for WLAN/WiMAX/Wi-Fi/Bluetooth/C-band applications," *AEU - Int. J. Electron. Commun.*, 2019,110, (3) p. 152871.